Journal of Biomolecular NMR, **22:** 175–179, 2002.
KLUWER/ESCOM

Measurement of conformational constraints in an elastin-mimetic protein by residue-pair selected solid-state NMR

Mei Hong[a,*], R. Andrew McMillan[b] & Vincent P. Conticello[b]
[a]*Department of Chemistry, Iowa State University, Ames, IA 50011, U.S.A.;* [b]*Department of Chemistry, Emory University, Atlanta, GA 30322, U.S.A.*

Received 10 October 2001; Accepted 26 November 2001

Key words: chemical shift anisotropy, elastin, protein conformation, selective and extensive labeling, SPECIFIC CP

Abstract

We introduce a solid-state NMR technique for selective detection of a residue pair in multiply labeled proteins to obtain site-specific structural constraints. The method exploits the frequency-offset dependence of cross polarization to achieve $^{13}CO_i \rightarrow {}^{15}N_i \rightarrow {}^{13}C\alpha_i$ transfer between two residues. A ^{13}C, ^{15}N-labeled elastin mimetic protein $(VPGVG)_n$ is used to demonstrate the method. The technique selected the Gly3 Cα signal while suppressing the Gly5 Cα signal, and allowed the measurement of the Gly3 Cα chemical shift anisotropy to derive information on the protein conformation. This residue-pair selection technique should simplify the study of protein structure at specific residues.

Structure determination of complex insoluble proteins by solid-state NMR usually requires site-specific labeling of ^{13}C, ^{15}N, or ^{2}H nuclei. While single-residue and single-site labeling is straightforward for small synthetic peptides, it is more challenging for an expressed protein, due to the usual presence of multiple copies of an amino acid in a protein. Often, selective but extensive isotopic labeling approaches that exploit the biosynthetic pathways and generic precursors such as glucose are simpler and more economical (Hong, 1999; Hong and Jakes, 1999). In the presence of multiple isotopic labels, it is desirable to select the signal of a specific residue spectroscopically, in order to measure its conformational or dynamical parameters without overlap from other resonances (Kikuchi and Asakura, 1999).

Here, we demonstrate the selection of the signal of a unique residue in a multiply ^{13}C and ^{15}N labeled protein using three sequential cross polarization (CP) steps (Pines et al., 1973). The recombinant protein, poly(Lys-25), has a repeat sequence of $[(VPGVG)_4(VPGKG)]_{39}$ and a molecular weight of 81 kDa (McMillian and Conticello, 2000; McMillian et al., 1999). It mimics the structure and properties of natural insoluble elastin, and is a promising material as artificial tissues and drug delivery agents (Huang et al., 2000; Urry, 1999). The protein was labeled uniformly in ^{15}N, but selectively and extensively in ^{13}C with [2-^{13}C] glycerol as the sole carbon source of the expression media. An examination of the biosynthetic pathways (Hong, 1999) indicates that this ^{13}C precursor yields $^{13}C\alpha$ and $^{13}C\beta$ labeled Val, $^{13}C\alpha$ labeled Gly and ^{13}CO, $^{13}C\alpha$, $^{13}C\beta$ and $^{13}C\delta$ labeled Pro (Figure 1). Lys is partially labeled at Cα, Cγ, Cδ and Cε. However, its rare occurrence in the protein (4% of the total residues) and the low labeling levels of its sidechain carbons (Hong, 1999) make the Lys ^{13}C signals negligible. This protein has been postulated to form a repeated β-turn structure termed β-spiral (Urry, 1997; Urry et al., 1989), with the Pro2-Gly3 pair at the center of each β-turn. This β-spiral motif is thought to underlie the elasticity of this class of proteins (Urry, 1988). While these conformers have been observed in the crystal structure of a model peptide cyclo-$(VPGVG)_3$ (Cook et al., 1980), recent mole-

*To whom correspondence should be addressed. E-mail: mhong@iastate.edu

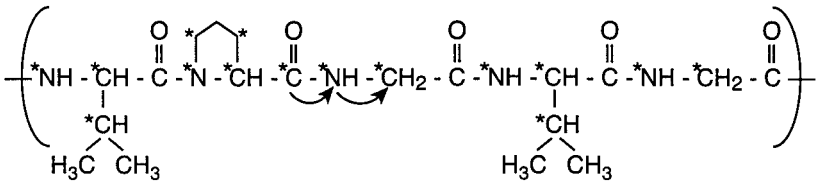

Figure 1. The main repeat sequence of poly(Lys-25), VPGVG, and its labeling scheme. Asterisks indicate the labeled sites in the protein. Arrows indicate the backbone spins involved in the triple-CP pathway. The protein was biosynthetically expressed (McMillian and Conticello, 2000) with [2-^{13}C] glycerol as the sole carbon source and ^{15}N-labeled ammonium chloride as the sole ^{15}N source.

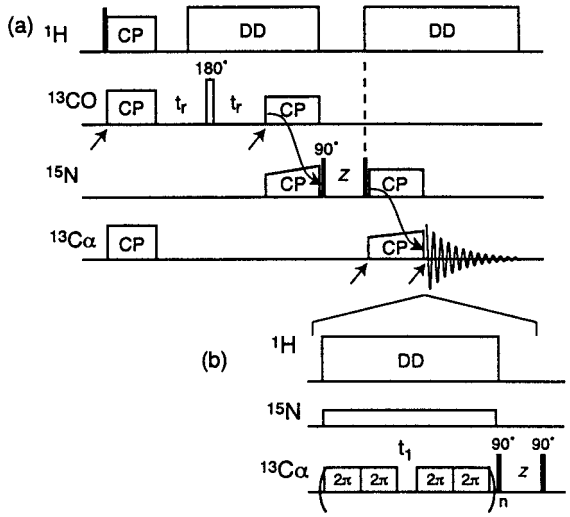

Figure 2. Pulse sequences for (a) residue-pair selection by triple CP, and (b) chemical shift anisotropy measurement after residue-pair selection. The ^{13}C carrier frequency is switched four times at time points represented by arrows. Sequentially, the ^{13}C carrier frequency is placed on-resonance for CO, Cα, CO, and Cα. The CSA recoupling period uses 2π pulses and is incremented at one rotor period per t_1 point (Liu et al., 2001).

cular dynamics simulations of $(VPGVG)_{18}$ in water have called into question the importance of the β-spiral structure and associated type-II β turns within the pentapeptide repeats of elastin above its transition temperature (Li et al., 2001). Thus, it would be structurally informative and physiologically relevant to obtain conformational constraints of Pro2 and Gly3 for an elastin-mimetic polypeptide in the condensed phase. However, the Cα peaks of the two Gly residues in each repeat sequence overlap exactly at 43.3 ppm, as shown in Figure 4a below, making it difficult to extract site-specific structural constraints. We show here that the residue-pair selection approach removes this resonance overlap, and permits the measurement of conformation-dependent chemical shift parameters at the critical Gly3 residue.

To selectively detect the Gly3 Cα signal, we take advantage of the unique ^{13}CO labeling of Pro2 afforded by the [2-^{13}C] glycerol labeling protocol. If the Pro2 CO magnetization is selected while all other ^{13}C signals are suppressed, and is transferred in two relayed steps, first to Gly3 ^{15}N and then to Gly3 Cα, then we should be able to detect the Gly3 Cα signal only. The Gly5 Cα signal would be removed by the initial suppression of the aliphatic carbons and by making the relayed CP steps frequency-specific (Baldus et al., 1998). The pulse sequence for this triple-CP experiment is shown in Figure 2a. After a standard broadband CP from ^{1}H to ^{13}C, a Hahn echo is applied on ^{13}C, during which the ^{1}H decoupling field is turned off for 40 μs. This suppresses the signals of all protonated carbons such as Cα while retaining the signal of the unprotonated carbonyl carbon. Since this ^{1}H-^{13}C CP is broadband, spin-lock is shown on both the ^{13}CO and the ^{13}Cα lines in the pulse sequence. Next, the selected Pro2 ^{13}CO magnetization is transferred to its directly bonded Gly3 ^{15}N by frequency-specific CP (Baldus et al., 1998; Rienstra et al., 2000). This is achieved by placing the ^{13}C carrier frequency away from the CO peak (174 ppm), in the Cα region (40–65 ppm), and choosing the ^{13}C spin-lock field strength, γB_1, to be comparable to the CO frequency offset of 15–20 kHz. As a result, the carbonyl carbon experiences an effective field, B_{eff}, that differs significantly from the transverse applied field B_1 in both direction and magnitude. The ^{15}N spin-lock field matches the CO effective field, but differs from the transverse field experienced by Cα, thus the inter-residue ^{13}CO–^{15}N transfer is optimized while the intra-residue ^{13}Cα–^{15}N transfer is minimized. A 10% ramp is applied on the ^{15}N channel, in order to avoid mismatch of the sharp CP condition.

After the second CP, the ^{15}N magnetization is stored along the z-direction for a rotor period while the ^{1}H decoupling is turned off. This dephases all transverse ^{13}C magnetization, thus ensuring that the finally detected ^{13}C signals originate from the ^{15}N

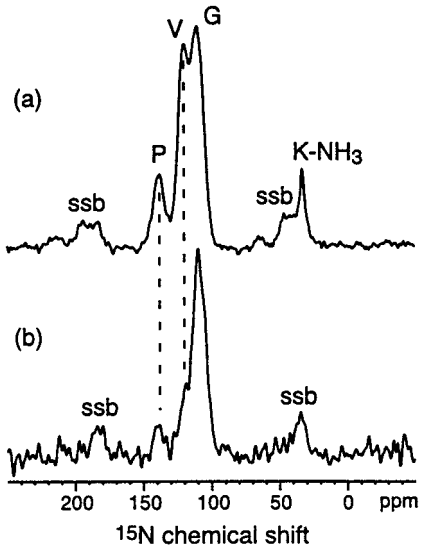

Figure 3. ^{15}N spectra of poly(Lys-25). (a) Standard ^{1}H–^{15}N CP spectrum. Number of scans (NS) = 1024. (b) Double ^{1}H–^{13}CO and ^{13}CO-^{15}N CP spectrum. NS = 23192. ssb: spinning sidebands. Contact times were 1.2 ms for ^{1}H-^{13}C CP and 3 ms for ^{13}C-^{15}N CP. 7.8 mg of the dry protein powder, hydrated to 20% by weight, was used in all experiments described here. The NMR spectra were acquired on a Bruker DSX-400 spectrometer (Karlsruhe, Germany) with a 9.4 Tesla magnet. The resonance frequencies are 400.49 MHz for ^{1}H, 100.7 MHz for ^{13}C, and 40.5 MHz for ^{15}N. A triple-resonance 4 mm MAS probe was used. All spectra were acquired at a spinning speed of 3 kHz. Typical rf field strengths were 80 kHz for ^{1}H decoupling, 50 kHz for ^{1}H-^{13}C CP, and 15–20 kHz for CP between ^{13}C and ^{15}N.

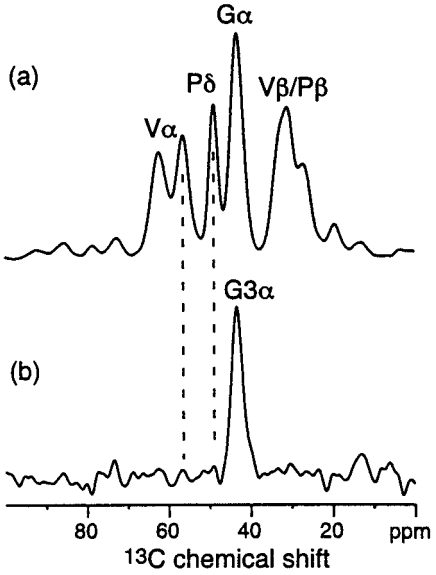

Figure 4. ^{13}C spectra of poly(Lys-25). (a) Standard CP (^{1}H-^{13}C) spectrum at 3 kHz MAS. NS = 16. (b) Triple-CP spectrum. NS = 1536. Contact times were 1.2 ms, 3 ms, and 3 ms for the three CP steps.

spin. During the third CP, the Gly3 ^{15}N magnetization is transferred to its directly bonded ^{13}Cα by using a large offset for Cα and matching the ^{15}N spin-lock field to the Cα effective field. Under this condition, the CO field strength differs from the ^{15}N field strength, thus back transfer from Gly3 ^{15}N to Pro2 ^{13}CO is suppressed. The weak ^{13}C ramp ($\sim$ 10%) during the third CP is insufficient to cause ^{15}N$\rightarrow$^{13}CO back transfer, as demonstrated by the extremely selective ^{13}C spectrum shown in Figure 4. Both the ^{13}CO$\rightarrow$^{15}N and ^{15}N$\rightarrow$^{13}Cα CP steps were conducted with spin lock field strengths of less than 20 kHz. The ^{1}H decoupling field strength during this time was about 80 kHz. Thus, there should be little leakage of magnetization to ^{1}H.

The frequency-specific CP from Pro2 ^{13}CO to Gly3 ^{15}N is demonstrated in Figure 3. The full ^{15}N magic-angle spinning (MAS) spectrum (Figure 3a) can be assigned based on the characteristic amino acid chemical shifts and 2D correlation experiments that will be described elsewhere. Except for the resolved Pro ^{15}N and Lys Nε peaks, the Val and Gly signals partially overlap. After 3 ms of ^{13}CO$\rightarrow$^{15}N CP, the ^{15}N spectrum (Figure 3b) shows only a Gly peak, while the Val, Lys, and Pro signals are nearly completely suppressed. The Gly peak must originate mostly from Gly3 and not from Gly5, since if residual Gly5 intensities were present due to incomplete suppression of the Cα signals and residual ^{13}Cα$\rightarrow$^{15}N transfer, then the same mechanisms should also retain the Val and Pro ^{15}N signals. The nearly complete absence of these peaks indicates that the intra-residue ^{13}Cα–^{15}N pathway is negligible. The small Pro ^{15}N signal is likely due to residual intra-residue two-bond transfer from Pro CO to Pro ^{15}N.

The ^{13}C-detected triple-CP experiment is demonstrated in Figure 4. The regular ^{13}C MAS spectrum (Figure 4a) shows that all peaks have partial overlap except for Pro Cδ. For instance, the broad resonance at about 60 ppm is the sum of two Val Cα signals and Pro Cα. The 30 ppm-peak combines two Val Cβ sites and Pro Cβ. Gly3 and Gly5 Cα sites both resonate at 43.3 ppm. After the relayed CP from ^{13}CO to ^{15}N and then to ^{13}Cα, only the Gly Cα signal remains (Figure 4b). Again, proof that this is due only to Gly3 and not Gly5 is made by comparison with other residues. If an intra-residue pathway such as ^{13}C$\alpha_i$$\rightarrow$^{15}N$_i$$\rightarrow$^{13}C$\alpha_i$ existed, then the Val and Pro Cα signals should also survive. Their complete absence in the spectrum shows unambiguously that the

43.3 ppm peak solely originates from Gly3. While the ^{15}N double-CP spectrum (Figure 3b) showed residual Pro ^{15}N intensity, the final step of frequency-specific CP completely removed the Pro Cα signal. This shows that the chemical shift difference of 17 ppm or 1.7 kHz between Gly Cα and Pro Cα is sufficient to eliminate ^{15}N→^{13}Cα CP within Pro. This illustrates the high specificity of the CP dynamics.

The efficiency of the triple-CP experiment is about 10% compared to the unfiltered ^{13}C CP experiment. This takes into account the fact that the Pro CO labeling level is at most 50% (Hong, 1999). Higher transfer efficiency can be achieved by increasing the ^{1}H decoupling field strength, especially during the two ^{13}C–^{15}N CP steps, and by spinning the sample faster. The double (^{15}N) and triple (^{13}C) CP spectra in Figures 3 and 4 was acquired at 3 kHz, in order to optimize the chemical shift anisotropy (CSA) measurement described below.

The selection of a unique Gly residue in a 1D experiment allows the addition of a second dimension to measure anisotropic interactions that contain structural information. Here, we chose to first measure the CSA of Gly3 Cα. Various experimental (Hong, 2000; Tjandra and Bax, 1997) and quantum-chemical calculations (Havlin et al., 1997) have shown that Cα CSAs are highly sensitive to protein backbone torsion angles. We used a recently developed technique involving 2π nutation pulses to recouple the CSA interaction quasi-statically under MAS (Liu et al., 2001). The additional pulses for this residue-pair selected CSA experiment are shown in Figure 2b. At the end of the triple-CP sequence, the selected ^{13}C signal evolves under the CSA interaction rotor synchronously for the t_1 period. The blocks of 2π pulses in each rotor period begin and end at times that were calculated previously by Tycko and coworkers to yield a static chemical shift powder pattern (Tycko et al., 1989). As a result of this time constraint, the field strength γB_1 of the 2π pulses is 12.12 times the spinning speed. Both ^{15}N and ^{1}H decoupling is applied during the CSA evolution, in order to remove the unwanted heteronuclear dipolar interactions. The use of 2π pulses, which are much less sensitive to rf field inhomogeneity than π pulses, yields undistorted CSA patterns, and reduces the ^{1}H decoupling requirement from a factor of 3 to a factor of 2 times the ^{13}C field strength (Liu et al., 2001). This CSA recoupling sequence also reintroduces the ^{13}C-^{13}C homonuclear dipolar coupling; however, this does not affect the CSA measurement of Gly ^{13}Cα here, which has no directly bonded ^{13}C neighbor.

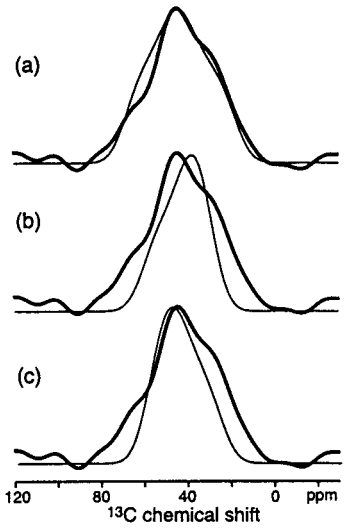

Figure 5. Experimental Gly3 Cα CSA spectrum (bold) after Pro2-Gly3 selection, extracted from the indirect dimension of the 2D CSA-recoupling spectrum. NS = 2592 for each t_1 slice. States detection was used to obtain pure absorptive CSA spectra (States et al., 1982). The t_1 period was incremented at 333 μs, or one rotor period. Twelve t_1 increments were measured, yielding a maximum evolution time of 4 ms. The experimental spectrum is superimposed with various simulations (thin lines). (a) Best-fit simulation, with $\Delta\sigma = 50$ ppm and $\eta = 0.93$. (b) Simulated β-sheet CSA ($\Delta\sigma = 32$ ppm, $\eta = 0.47$). (c) Simulated α-helical CSA ($\Delta\sigma = 34$ ppm, $\eta = 0.61$).

The t_1 time signal is amplitude-modulated with the States method (States et al., 1982), and ^{13}C isotropic chemical shifts are detected in t_2.

The quasi-static recoupled CSA pattern of Gly3 Cα, extracted from the indirect dimension of the 2D spectrum, is shown in Figure 5a. It is best fit with an anisotropic span ($\Delta\sigma = |\sigma_{33} - \sigma_{11}|$) of 50 ppm and an asymmetry parameter of 0.93. Within experimental uncertainty, this agrees well with the calculated CSA parameters for both type-I β-turn ($\Delta\sigma = 49$ ppm, $\eta = 0.86$) and type-II β-turn ($\Delta\sigma = 47$ ppm and $\eta = 0.87$) (Havlin et al., 1997). However, the experimental CSA value is much larger than the quantum-chemically calculated CSAs for either β-sheet or α-helical conformations: the former has $\Delta\sigma = 32$ ppm and $\eta = 0.47$, while the corresponding values for α-helices are 34 ppm and 0.61 (Figures 5b and 5c) (Havlin et al., 1997). These deviations are many times larger than the experimental uncertainty. Therefore, we can confidently rule out the β-sheet and α-helical conformations for Gly3. Rather, the Gly3 CSA is consistent with a β-turn structure, whose specific de-

tails will be further measured using torsion angle and distance constraints.

This triple-CP technique for residue-pair selection should be useful for investigating the detailed structure of proteins at specific residues. It selects a pair of residues by three frequency-specific CP steps, thus significantly reducing the amino acid multiplicity in a polypeptide chain. To use this approach, one can combine a ^{13}CO-labeled amino acid type with a ^{15}N and ^{13}Cα labeled residue type in the protein expression. Alternatively, selective and extensive ^{13}C labeling approaches involving few CO labels (Hong, 1999) can be exploited to yield the desired ^{13}C distribution. It has been shown that suitable choice of the ^{13}C precursor can give very sparse CO labeling patterns in proteins (Hong, 1999). For example, [2-^{13}C] glycerol combined with inhibition of the citric-acid-cycle amino acids gives Leu as the only CO-labeled residue. TEASE labeling starting from [1-^{13}C] glucose will give His as the only ^{13}CO-labeled residue. Thus, there are many possibilities for generating proteins with only a few ^{13}CO labels, providing a flexible means of residue-pair selection.

It should be realized that due to the conformation dependence of isotropic chemical shifts, the Cα signals of each residue type are often partly resolved. Thus, it may not always be necessary to have a chemically unique residue pair to apply this triple-CP technique. The Gly example shown here represents the most challenging case of resonance overlap. The use of frequency-offset dependence in pulse sequence design (Egorova-Zachernyuk et al., 2001; Jaroniec et al., 2001; Nomura et al., 2000; Rienstra et al., 2000; Takegoshi et al., 1995, 1997) opens many possibilities for resonance assignment and structure determination of solid proteins. The efficiency of this triple-CP polarization transfer is sufficient to be incorporated into a 2D experiment to extract useful structural constraints such as the CSA, and combinations with torsion angle measurements can be readily envisioned.

Acknowledgements

M.H. thanks the Arnold and Mabel Beckman Foundation for a Young Investigator Award and the National Science Foundation for a CAREER award (MCB-0093398). The work at Iowa State University is supported by a Biotechnology Grant and a Starter Grant. V.P.C acknowledges NASA for support (NAG8-1579).

References

Baldus, M., Petkova, A.T., Herzfeld, J. and Griffin, R.G. (1998) *Mol. Phys.*, **95**, 1197–1207.

Cook, W.J., Einspahr, H., Trapane, T.L., Urry, D.W. and Bugg, C.E. (1980) *J. Am. Chem. Soc.*, **102**, 5502–5505.

Egorova-Zachernyuk, T.A., Hollander, J., Fraser, N., Gast, P., Hoff, A.J., Cogdell, R., Groot, H.J.d. and Baldus, M. (2001) *J. Biomol. NMR*, **19**, 243–253.

Havlin, R.H., Le, H., Laws, D.D., deDios, A.C. and Oldfield, E. (1997) *J. Am. Chem. Soc.*, **119**, 11951–11958.

Hong, M. (1999) *J. Magn. Reson.*, **139**, 389–401.

Hong, M. (2000) *J. Am. Chem. Soc.*, **122**, 3762–3770.

Hong, M. and Jakes, K. (1999) *J. Biomol. NMR*, **14**, 71–74.

Huang, L., McMillan, R.A., Apkarian, R.P., Pourdeyhimi, B., Conticello, V.P. and Chaikof, E.L. (2000) *Macromolecules*, **33**, 2989–2997.

Jaroniec, C.P., Tounge, B.A., Herzfeld, J. and Griffin, R.G. (2001) *J. Am. Chem. Soc.*, **123**, 3507–3519.

Kikuchi, J. and Asakura, T. (1999) *J. Biochem. Biophys. Meth.*, **38**, 203–208.

Li, B., Alonso, O.V. and Daggett, V. (2001) *J. Mol. Biol.*, **305**, 581–592.

Liu, S.F., Mao, J.D. and Schmidt-Rohr, K. (2001) *J. Magn. Reson.*, in press.

McMillian, R.A. and Conticello, V.P. (2000) *Macromolecules*, **33**, 4809–4821.

McMillian, R.A., Lee, T.A.T. and Conticello, V.P. (1999) *Macromolecules*, **32**, 3643–3648.

Nomura, K., Takegoshi, K., Terao, T., Uchida, K. and Kainosho, M. (2000) *J. Biomol. NMR*, **17**, 111–123.

Pines, A., Gibby, M.G. and Waugh, J.S. (1973) *J. Chem. Phys.*, **59**, 569–590.

Rienstra, C.M., Hohwy, M., Hong, M. and Griffin, R.G. (2000) *J. Am. Chem. Soc.*, **122**, 10979–10990.

States, D.J., Haberkorn, R.A. and Ruben, D.J. (1982) *J. Magn. Reson.*, **48**, 286–292.

Takegoshi, K., Nomura, K. and Terao, T. (1995) *Chem. Phys. Lett.*, **232**, 424–428.

Takegoshi, K., Nomura, K. and Terao, T. (1997) *J. Magn. Reson.*, **127**, 206–216.

Tjandra, N. and Bax, A. (1997) *J. Am. Chem. Soc.*, **119**, 9576–9577.

Tycko, R., Dabbagh, G. and Mirau, P. (1989) *J. Magn. Reson.*, **85**, 265–274.

Urry, D.W. (1988) *J. Prot. Chem.*, **7**, 1–34.

Urry, D.W. (1997) In *On the Molecular Structure, Function and Pathology of Elastin: The Gotte Stepping Stone*, Tamburro, A.M. (Ed.), Armento, Potenza, Italy, pp. 11–22.

Urry, D.W. (1999) *Trends Biotechnol.*, **7**, 249–257.

Urry, D.W., Chang, D.K., Krishna, N.R., Huang, D.H., Trapane, T.L. and Prasad, K.U. (1989) *Biopolymers*, **28**, 819–833.